EVALUATION OF MECHANICAL PROPERTIES OF LOW COST FMLs FABRICATED WITH COIR FIBRE-REINFORCED COMPOSITES

Júlio C. dos Santos[1], Luciano M. G. Vieira[2], Rodrigo T. S. Freire[1,3], André L. Christoforo[4], Juan C. C. Rubio[2], Túlio H. Panzera[1].

[1] Centre for Innovation and Technology in Composite Materials, Department of Mechanical Engineering, Federal University of São João del Rei, Brazil.

[2] Department of Production Engineering, Federal University of Minas Gerais, Brazil.

[3] Department of Natural Sciences, Federal University of São João del Rei, Brazil.

[4] Federal University of São Carlos (UFSCar), Department of Civil Engineering, São Carlos, Brazil.

https://doi.org/10.21452/bccm4.2018.07.04

ABSTRACT: Fibre Metal Laminates (FMLs) are composite structures that comprise alternating metal layers and fibre-reinforced polymer composites (FRCs) combining their distinct physical-mechanical properties. Traditional FMLs are based on synthetic (carbon, glass and aramid) fibres. However, alternative FMLs based on natural fibre-reinforced composites have been developed to take advantage of available natural resources. A new eco-friendly FML sandwich based on random coir fibre-reinforced epoxy and polyester resin was developed in this research. Mechanical tests revealed that the tensile properties were fully dominated by the aluminium sheets, which were treated with alkali for degreasing and wash primer in order to enhance interfacial bonding. Such treatment efficiently reduced delamination and increased the flexural modulus (~67%). A similar increase in flexural (~22.94%) and impact strength (~99.16%) as well as in skin stress (~20.89%) of the new FMLs proposed was observed owing to the flexural and impact strength of composite cores and better core-layer stress transfer upon the aluminium treatment.

keywords: FML-sandwich composites, epoxy, polyester, coir fibre, mechanical properties.

1. INTRODUCTION

Fibre Metal Laminates (FMLs) are composite structures that comprise alternating metal layers and fibre-reinforced polymer composites (FRCs) combining their distinct physical and mechanical properties. As a result, the new structures have advantages over conventional fibre-reinforced composites, e.g. sustainability, resistance to fatigue, corrosion and impact [1]. ARALL, GLARE and CARAAL are traditional FMLs with synthetic fibre-based cores (carbon, glass and aramid fibres) [2]. However, alternative cores based on natural fibre-reinforced composites [3][4][5][6] have been developed due to increasing environmental concerns in order to take advantage of the available natural resources FMLs may be

manufactured with metallic faces composed of magnesium [1], titanium [7] , and a variety of aluminum alloys such as 2024-T3[6][8], 7075-O[9], 6061-O and T3[9] and aluminum-lithium[10]. The mechanical properties and thence the final applications of the FML depend on the selected metallic face and core. Vieira *et al*. [6] investigated the mechanical properties of a sisal fibre composite core FML with aluminium 2024-T3 faces and obtained ~23 GPa and 205 Mpa for flexural modulus and strength, respectively. These figures rank Vieira's material a promising FML for structural engineering applications.

FMLs can also be recognized as sandwich structures. In all FML applications, face-core bond strength is a fundamental property [11]. The mechanical efficiency of FMLs is indeed determined by the ability of this interfacial region to transfer mechanical loads through the constituents materials [4][5][6][12][10][3]. Thus, pre-treatments of aluminum faces are important to improve the inherently weak interlaminar bond strength between the aluminum alloy and the polymeric core [11][12][6].

The purpose of this work is to study an FML sandwich made of coir fibre-reinforced epoxy (CFREP) and polyester (CFRPO) composite cores, sandwiched to aluminium alloy ISO 1200 faces. A simple treatment method was used for aluminium faces in order to increase their consolidation with polymeric resins but an additional wash primer treatment was performed on the metallic sheets when polyester resin was used. The new eco-friendly FML sandwiched structure named CoRAL (Coir fibre-Reinforced ALuminium sheets) was evaluated under tensile, flexural and impact tests and its density was also determined.

2. EXPERIMENTAL PROCEDURES

2.1 Materials

CoRAL FML consists of two 0.5 mm-thick aluminium faces adhered to a coir-reinforced epoxy (or polyester) composite cores. The epoxy resin (Renlam M) and the amine-based hardener (Aradur HY 956) were provided by Huntsman (Brazil). The unsaturated polyester resin and Metil Ethil Ketone (2 wt%) were supplied by Reichhold (Brazil). Wash primer, (Sherwin Williams Automotive Finishes), was used as a coat sealant for aluminium. The raw coir fibre mat and aluminium sheets 1200-H14 (type ISO 1200) were obtained from Deflor Bioengenharia and Belmetal (Brazil), respectively.

2.2 Fabrication

CoRALs and their cores were produced were produced by hand lay-up with uniaxial cold compression. The fabrication was a two-step process, basically as described by [13].

1st step: Aluminium treatment

Coir fibre-reinforced polymer composites (CFRPCs) were manufactured by treating the surface of the aluminium moulding plates with *Tec Glaze-N* mould release agent to ensure eficient demoulding of the composite samples.

For CoRAL, the surface treatment of aluminium alloy faces was performed as follows: 1) washing with a surfactant; 2) mechanical abrasion with 150 sandpaper grit so as to produce a pattern of mutually perpendicular slots oriented at ± 45°; 3) alkaline degreasing with 5 wt% NaOH solution to promote the *"Bridging effect"* [11]; 4) priming - wash primer was applied by a compressed air spray gun. Two layers were successively applied with a 10 min interval.

It is worth noting that water molecules do not uniformly cover the surface of aluminium sheets washed only with surfactant (an effect known as "water breaking") (Figure 1a), due to remaining oil and other hydrophobic contaminants. These are subsequently removed by the alkaline-degreasing process, which results in the uniform film of water shown in Figure 1b. The alkaline treatment prepares the surface for the wash primer application (Figure 1c).

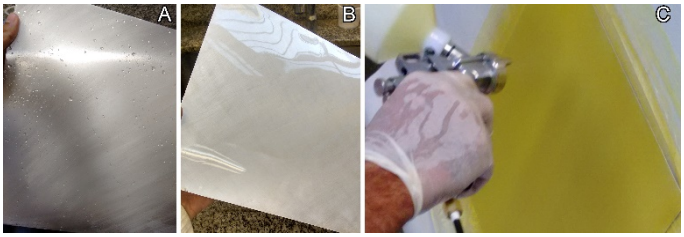

Figure 1. Aluminium treatment: a) water break after washing with surfactant and b) uniform film of water formed after mechanical abrasion with alkaline degreasing; c) wash primer application.

2nd step: Hand Lay-up manufacturing

After the first aluminium plate has been laid on the metallic mould (300 x 300 x 4 mm), the coir fibre mat (900 g/cm^2) along with the polymeric mixture (30/70 fibre-matrix volume fraction) was added (Figure 2a). The second aluminium face was then laid and the metallic mould was closed, as schematically shown in Figure 2b. The laminates were pressed in a hydraulic press under 645 KPa. To ensure the desired sample thickness, two steel bars (1 inch) were bolted over the top mould, Figure 2c, and the compaction load was released. After 60 hours, the FML was removed from the mould and cured for 14 days, period after which the laminates were cut (Figure 2d) and tested.

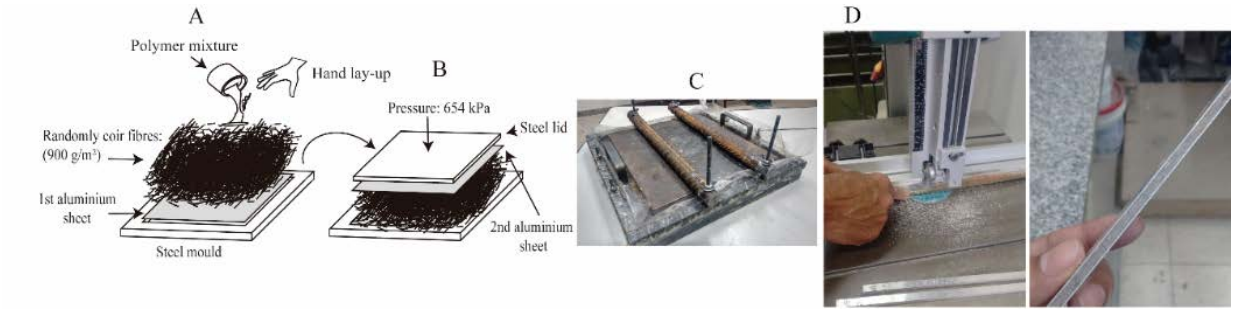

Figure 2. Manufacturing process.

2.3 Statistical analysis

Six (6) experimental conditions were considered for CoRALs based on the treatments decribed in Table 1. The sample code attributed to epoxy and polyester-based CoRALs is presented in Table 1.

Table 1. Experimental conditions investigated for CoRAL.

Aluminium treatment	Epoxy	Polyester
Untreated	E1	P1
Sandpapered-NaOH	E2	P2
Sandpapered-NaOH/wash primer	E3	P3

The analysis of variance (ANOVA) was conducted to investigate the main effects of the selected factors on the mechanical response variables considered. ANOVA is essentially a hypothesis test that considers the equivalence among mean values as the null hypothesis. The P-value, which is the risk of rejecting the null hypotheses (no effect from the main factor or interaction) when the null hypothesis is in fact true, is then calculated. In this work, the effect is considered statistically significant for $P \leq 0.05$. The Anderson–Darling test was used to verify the normality of the data distribution and validate the ANOVA. Though ANOVA identifies that means are statistically different, it does not determine which means are

statistically different. Tukey's multiple comparison test was used for this task, so that means that do not share the same letter coding are significantly different, as will be shown below.

2.4 Mechanical and physical tests

Composite core (CFRPCs) as well as CoRALs were evaluated under tensile tests (TT) with rectangular specimens (250 x 25 mm) according to ASTM D3039[14]. Flexural tests (FT) of CFRPCs were performed in accordance to ASTM D790 (2015)[15]. CoRAL samples were tested under three-point bending tests according to ASTM D7249 (2012) recommendations [16]. These tests were performed on a Shimadzu AGX-Plus universal testing machine equipped with a 100 kN load cell. Edgewise Charpy Impact Strength tests (CIS) were performed in an XJJ- series impact testing machine with a 15 J hammer following ISO 179-1 (2010)[17], with samples of dimensions 80 x 10 x 4 mm. Tests were performed at 23 C and humidity level of 55%.

Equations 1 and 2 presented below represent a simple and consistent approach to determine the tensile normal stress to which each element (core or faces) are submitted. Assuming linear elasticity, the tensile yield load (in N) was divided by the cross-sectional area of the individual element to determine the average normal stress (σ), given by Equation 1 (aluminium face normal stress) and Equation 2 (composite core normal stress). The load at yield point was measured considering 2% deformation/strain.

$$\sigma_{al} = \frac{E_{al} \cdot F}{E_{al} \cdot S_{al} + E_c \cdot S_c} \quad (1)$$

$$\sigma_c = \frac{E_c \cdot F}{E_{al} \cdot S_{al} + E_c \cdot S_c} \quad (2)$$

In these equations, E_{al} stands for the aluminium tensile modulus and E_c for the composite tensile modulus. The parameter F is the tensile load at yield point and S_c and S_{al} are the cross-sectional areas of composite and aluminium faces, respectively.

According to the theory of laminated beams [18], the effective flexural modulus of the laminate composite (E_f) can be expressed as shown in Equation 3, where E_x is the composite modulus (GPa) and the coordinates $Z_j - Z_{j-1}$ define a generic layer (Figure 3). Once the effective flexural modulus has been calculated, the normal stress through the FML thickness may determined by Equation 4. This theory assumes the "*pure flexure"* or, in other words, the linear elastic state. Equation 4 considers the flexural yield load (N), based on 2% deformation/strain.

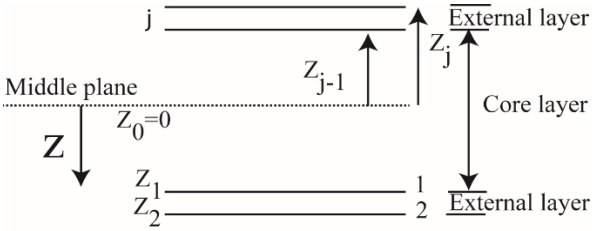

Figure 3. Distribution of generic layers of a 3 layers composites.

$$E_f = \frac{8}{t^3} \sum_{j=1}^{N/2} (E_x)_j \left(z_j^3 - z_{j-1}^3\right) \quad (3)$$

$$(\sigma_x)_j = \frac{MF.z}{I_{yy}} \left[\frac{(E_x)_j}{E_f}\right] \quad (4)$$

Fractographic analysis of the laminates was performed using an optical microscope. The density of CoRALs was also calculated by dividing the mass of the samples by the measured volume of the specimens. FMLs were also characterized by their metal volume fraction (MVF), defined as (Vlot and Gunnink, 2001) [6], [19]:

$$MVF = \frac{\sum_1^n t_{\text{metal (the thickness of total aluminium layer)}}}{t_{\text{laminated(thickness of total fml)}}} \quad (3)$$

3 RESULTS AND DISCUSSION

3.1 Physical and mechanical properties of cores and face

The results of the physical and mechanical properties of the core (CFREP and CRFPO) and face (1200 aluminium sheets) are listed in Table 2. The bases for the differences in the mechanical properties between the two coir-derived composites have been explored in another investigation, published elsewhere [20], and, therefore, are not described here.

Table 2. Physical and mechanical properties of CFRPCs and aluminium faces.

Material (isolated elements)		Tensile		Flexural		Impact	Density
		Mod.	Str.	Mod.	Str.	Str.	
		GPa	MPa	GPa	MPa	kJ/m²	g/cm³
Core	CFREP	2.33 (0.14)	17.48 (0.74)	2.27 (0.09)	34.90 (5.16)	6.04 (0.74)	1.03 (0.01)
	CFRPO	2.50 (0.07)	12.50 (1.11)	2.38 (0.13)	24.73 (3.61)	18.03 (2.37)	1.07 (0.03)
Face	AL. 1200	44-60	115-136	-	-	-	2.70

3.2 Demoulding and cutting process

CoRAL samples P1 and P2 presented delamination upon demoulding and/or cutting process. Due to poor consolidation with the polyester resin, mechanical tests for these conditions were not performed.

3.3 Physical properties of CoRAL: density and MVF

The density of CoRAL samples varied from 1.27 to 1.37 g/cm³. The density of epoxy based CoRALs increased 30% if compared to CFREP (1.03 g/cm³) and, 28.97% (CoRAL P3) compared to CFRPO (1.07 g/cm³).

Table 3. Physical properties of CoRAL.

Properties	*Coral E1*	*Coral E2*	*Coral E3*	*Coral P3*
Density (g/cm³)	1.37(0.08)	1.37(0.08)	1.28(0.05)	1.38(0.03)
Metal volume fraction (MVF)	24.11%	25.15%	23.00%	24.50%

With 23% of aluminium volume fraction, CoRAL E3 tended to present the lowest density value due to low aluminium volume fraction. The metal volume fraction shows that the addition of aluminium plates (2.7 g/cm³) contributed to an increase in density compared to coir-derived composites. Similar results were obtained in [6].

3.4 Tensile tests

Table 4 presents the mean tensile properties for CoRALs. No statistical significance was found for maximum tensile strength, since a p-value of 0.301 was obtained, indicating that the means of tensile strength are equal for all the conditions considered.

The post-yield linear part of tensile stress-strain curves for FMLs only depends on the stiffness of the core [21]. After yield point the aluminium face stress (extremely higher than CFREP and CFRPO – see Table 4), is suddenly transferred to the core resulting in catastrophic failure. No significant improvement was therefore obtained for maximum tensile strength of CoRAL samples.

Table 4. Mean of tensile properties of CoRAL samples.

Properties	*Coral E1*	*Coral E2*	*Coral E3*	*Coral P3*
Max. tensile strength (MPa)	36.88(1.93)	37.71 (2.00)	37.11(0.61)	36.08(1.90)
Core tensile yield strength (MPa)	5.83(0.09)	5.93(0.44)	6.02(0.41)	6.54(0.35)
Face tensile yield strength (MPa)	108.77(1.67)	110.74(8.24)	112.38(7.70)	111.17(6.07)

Typical stress-strain curves and fractographic analyses and failure modes observed after the tensile tests are presented in Figure 4. After unloading CoRAL E1 (see Figure 4 item CoRAL E1) presented delamination and plastic deformations of both faces between the CFREP and aluminium layers, resulting of shear stresses in the interfacial plane and the energy dissipated at the moment of failure, caused by poor interface [21], [22]. Once maximum stress is achieved, a brittle fracture mode in the composite layers was observed, as well as fibre pull-out.

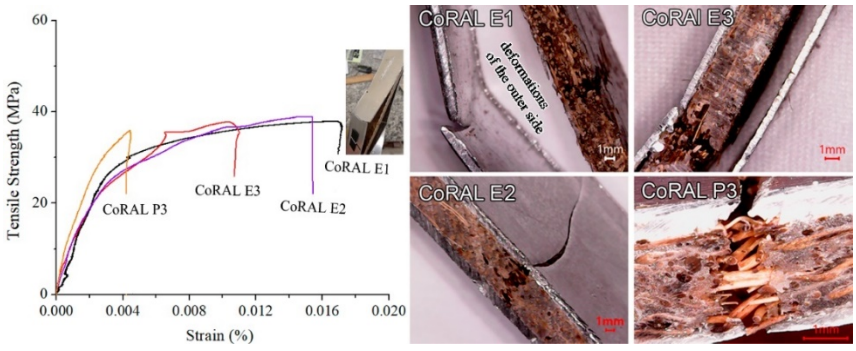

Figure 4. Tensile test: left) stress/strain curves right) morphologies of failure.

3.5 Three-point bending tests

3.5.1 Flexural modulus and strength

The flexural modulus ranged from 18.18 to 30.44 GPa (Table 5). The p-value for ANOVA was 0.024, indicating that the mean values for flexural modulus are significantly different.

According to Tukey's test (see Table 5), the lowest flexural modulus value is attributed to CoRAL E1 samples. The increase of MVF contributes to improve flexural modulus. However, the appropriate surface preparation is essential to provide higher stiffness to FMLs [23]. Poor consolidation, due to chemical differences between inorganic aluminium faces and the organic polymer matrix core, resulted in a weak interface (see Figure 5 item CoRAL E1) and may explain the reduction in flexural properties.

The flexural strength of CoRALs varied from 83.92 to 103.17 MPa. CoRAL E2 presented the highest value for flexural strength (Table 5). The strength of CoRALs is strongly affected by the aluminium-core interaction, which is sensitively improved by the surface treatment used for CoRAL E2 samples. The specific flexural strength was also higher for CoRAL E2 (75.30 MPa).

Table 5. Mean of three-point bending test of CoRAL samples.

Properties	Flexural modulus (GPa)		Flexural strength (MPa)		Specific flexural strength ($MPa/g.cm^{-3}$)
	Mean	Tukey	Mean	Tukey	
CoRAL E1	18.18 (2.17)	C	83.92 (10.83)	C	61.25
CoRAL E2	30.44 (2.07)	A	103.17 (3.30)	A	75.30
CoRAL E3	24.07 (1.60)	B	90.55 (3.39)	B	70.74
CoRAL P3	27.13 (3.62)	A	89.25 (5.05)	B	64.67
ANOVA	*0.024*		*0.000*		-

Figure 5 (right side) depicts the interface evolution after aluminum treatment. After the linear state, the flexural behaviour of CoRALs shows the plasticity region due to the plastic deformation of the aluminium sheets – see Figure 5 (left side)[24]. When the CoRAL beam side submitted to tensile stress reaches failure, cracks initiate in the coir composite core which fails with a sudden load drop. Delamination in the aluminium-core interface was observed in CoRAL E1 (both sides) and E3 (side under tensile stress). Cracks in the aluminium face under tensile stress and through the core were the predominant failure modes in CoRAL E2 and P3. The failure of lower layers (submitted to tensile stress) greatly influences the flexural behaviour over other failures modes[24]. This effect is induced by the interfacial adhesion with the aluminium faces.

The comparison between CoRAL E2 and E3 (Table 5 and Figure 5) implies that the"*bridging effect*" (for more detail see ref. [11]) is more important than the wash primer treatment for epoxy based CoRALs. However, for polyester based CoRALs, the wash primer treatment was the only one able to provide an effective face-core consolidation. The reactions of wash primer bonding and curing are complex and many different reactions take place being unique for this chemistry[25].

An increase in the interfacial bonding with aluminium improves the maximum flexural load transfer, see Figure 5 (left side) [3][4][5][6][12][10]. Even with an effective aluminium-core bonding, the flexural strength of CoRAL P3 was only ~86% of CoRAL E2 and similar to CoRAL E3. However, experimental results showed that the flexural strength of composite cores also contributed to increase face-core load transfer. Such behaviour will be discussed in the following section.

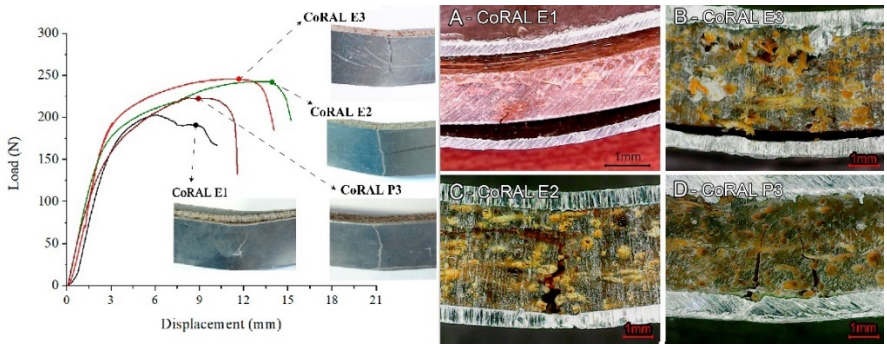

Figure 5. Flexural behaviour and failure mode for the CoRAL.

3.5.2 Normal stress distribution

The predicted stress distribution along the thickness of the CoRAL samples is presented in Figure 6. One can observed that the maximum normal stress occurs on the aluminium surface, Figure 5. The maximum stress occurs in the element with the higher modulus (aluminium faces - Table 2)[18].

As presented in Table 2, the flexural strength of CFREP (34.90 MPa) is ~41% higher than CFRPO (24.73 MPa). This explains why CoRAL P3 presented the lowest normal stress value at the Z_1(core) region (Table 6). However, the normal stress at Z_1(face) of the CoRAL E1 was the lowest of all other epoxy conditions. As previously reported, without treatment, a weak interfacial bonding takes place between aluminium sheets and the epoxy composite core. The load transferred between aluminium layers was reduced affecting the core stress. Owing to these effects, at Z_2(face) the stress of CoRAL E2 and E3 was superior than CoRAL E1 and P3.

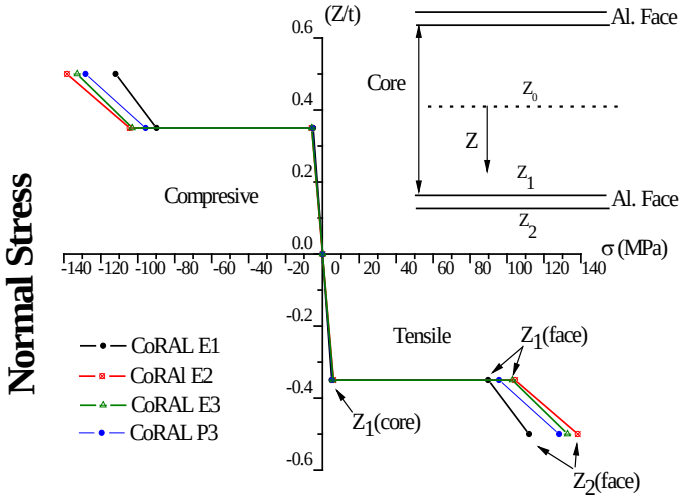

Figure 6. Normal stress distribution along the thickness of FML.

Table 6. Mean of normal stress (MPa) distribution along the thickness of CoRAL

Condition	Yield load						Max. load	
	Z_1(core)		Z_1(face)		Z_2(face)		Skin stress	
	Mean	Tukey	Mean	Tukey	Mean	Tukey	Mean	Tukey
CoRAL E1	5.24 (0.58)	AB	89.14 (5.02)	B	114.22 (7.99)	B	128.59 (14.54)	B
CoRAL	5.83	A	104.16	A	135.55	A	155.45	A

E2	(0.19)		(3.43)		(2.77)		(7.76)	
CoRAL E3	5.66 (0.18)	AB	101.17 (3.22)	A	134.96 (4.09)	A	146.44 (3.40)	AB
CoRAL P3	5.16 (0.29)	B	93.08 (4.04)	B	123.61 (5.57)	B	135.83 (9.29)	AB
ANOVA	*0.028*		*0.002*		*0.004*		*0.021*	

The superior skin stress for the experimental conditions was obtained for CoRAL E2. Experimental evidences based on the theory of laminated beams, imply the increase of CoRAL flexural behaviour is been induced by two factors: 1) interfacial bonding between aluminum and cores and 2) flexural strength of composite cores, which contributed to increase the load transfer.

3.6 Charpy impact test

The impact strength (Table 7) ranged from 32.33 to 64.39 kJ/m² for CoRAL E2 and CoRAL P3, respectively. The obtained p-value (0.001) reveals that the considered conditions significantly affected the impact strength and Tukey's test shows that the superior impact strength is attributed to CoRAL P3.

Table 7. Mean of impact test of CoRAL samples and Tukey's test.

Conditions	Impact Strength (kJ/m²)	
	mean	Tukey
CoRAL E1	a.d.c	-
CoRAL E2	32.33 (3.83)	B
CoRAL E3	36.40 (2.32)	B
CoRAL P3	64.39 (7.82)	A
ANOVA	*0.001*	
a.d.c* - aluminium debonding on cut.		

For FML sandwiches, crack propagation in the skin-core interface and through the core was responsible for the material failure [1]. In the epoxy and polyester CoRALs, fibre fracture and both aluminium and matrix fractures were observed (see Figure 7). The energy released with crack initiation or fracturing needs to be dissipated via various mechanisms. Fibre bridging and pull-out is one of the dominant methods of post-impact energy dissipation [1].

The loads from the cracking metal layers were transmitted via the adhesive to the fibres, thus unloading the metal layers and slowing down crack growth in these layers. The adhesive bonding between metal and composite core also plays an important role in the impact response of CoRAL. The impact strength of CFRPO (18.03 kJ/m³) was 198.51% higher than CFREP (6.04 kJ/m³). As a result, CoRAL P3 sandwich structure was found to have more efficient energy absorbing properties compared to CoRAL E1 and E2 under impact loading, because the coir fibre reinforced polyester core can dissipate more energy under impact load [20].

Figure 7. Post-impact fracture.

4 CONCLUSIONS

In this paper, the physical and mechanical properties of CoRALs were discussed. The tensile tests revealed that the metal layers control the tensile strength properties. No increase in tensile strength was obtained since the maximum tensile strength of composites cores was far below the maximum strength of aluminium. Different characteristic failure modes due to adhesive interface for the sandwich composites were found. The improvement of the interfacial adhesion between aluminium sheets and the composites cores was the major factor to increase the flexural load transfer and impact strength behaviour. The flexural behaviour can be described by two behaviours involving core flexural strength and interfacial aluminium/core shear transfer improved by aluminium treatment. With a good interface CoRAL-E showed superior flexural strength than CoRAL-P due to coir epoxy composites cores exhibiting greater flexural strength than polyester composites. However, CoRAL-P has superior impact behaviour than other currently available CoRALs, once coir polyester composites core has superior impact strength than coir epoxy ones.

ACKNOWLEDGMENTS

The authors would like to thank the Brazilian Research Agencies, CNPq, Fapemig and CAPES, for the financial support provided.

REFERENCES

[1] R. Das, A. Chanda, J. Brechou, and A. Banerjee, *17 – Impact behaviour of fibre–metal laminates*, no. February. Elsevier, 2016.

[2] T. Sinmazçelik, E. Avcu, M. Ö. Bora, and O. Çoban, “A review: Fibre metal laminates, background, bonding types and applied test methods,” *Mater. Des.*, vol. 32, no. 7, pp. 3671–3685, 2011.

[3] H. T. N. Kuan, W. J. Cantwell, M. a. Hazizan, and C. Santulli, “The fracture properties of environmental-friendly fiber metal laminates,” *J. Reinf. Plast. Compos.*, vol. 30, no. 6, pp. 499–508, 2011.

[4] J. Y. Zhang, T. X. Yu, J. K. Kim, and G. X. Sui, “Static indentation and impact behaviour of reformed bamboo/aluminium laminated composites,” *Compos. Struct.*, vol. 50, no. 2, pp. 207–216, 2000.

[5] C. Santulli, H. T. Kuan, F. Sarasini, I. De Rosa, and W. J. Cantwell, “Damage characterisation on PP-hemp/aluminium fibre–metal laminates using acoustic emission,” *J. Compos. Mater.*, vol. 47, no. 18, pp. 2265–2274, 2013.

[6] L. M. G. Vieira, J. C. dos Santos, T. H. Panzera, J. C. C. Rubio, and F. Scarpa, “Novel fibre metal laminate sandwich composite structure with sisal woven core,” *Ind. Crops Prod.*, vol. 99, pp. 189–195, 2017.

[7] H. Li, Y. Hu, C. Liu, X. Zheng, H. Liu, and J. Tao, “The effect of thermal fatigue on the mechanical properties of the novel fiber metal laminates based on aluminum-lithium alloy,” *Compos. Part A Appl. Sci. Manuf.*, vol. 84, pp. 36–42, 2016.

[8] H. Ahmadi, G. H. Liaghat, H. Sabouri, and E. Bidkhouri, “Investigation on the high

velocity impact properties of glass-reinforced fiber metal laminates," *J. Compos. Mater.*, vol. 47, no. 13, pp. 1605–1615, 2013.

[9] J. Zhou, Z. W. Guan, and W. J. Cantwell, "The influence of strain-rate on the perforation resistance of fiber metal laminates," *Compos. Struct.*, vol. 125, pp. 247–255, 2015.

[10] B. Yu, P. He, Z. Jiang, and J. Yang, "Interlaminar fracture properties of surface treated Ti-CFRP hybrid composites under long-term hygrothermal conditions," *Compos. Part A Appl. Sci. Manuf.*, vol. 96, pp. 9–17, 2017.

[11] W. Wu, D. Abliz, B. Jiang, G. Ziegmann, and D. Meiners, "A novel process for cost effective manufacturing of fiber metal laminate with textile reinforced pCBT composites and aluminum alloy," *Compos. Struct.*, vol. 108, no. 1, pp. 172–180, 2014.

[12] P. R. Oliveira, A. M. S. Bonaccorsi, T. H. Panzera, A. L. Christoforo, and F. Scarpa, "Sustainable sandwich composite structures made from aluminium sheets and disposed bottle caps," *Thin-Walled Struct.*, vol. 120, no. April, pp. 38–45, 2017.

[13] L. A. . OLIVEIRA, J. C. . SANTOS, T. H. . PANZERA, R. T. . FREIRE, L. M. G. . VIEIRA, and SCARPA, "Evaluation of Hybrid-Short-Coir-Fibre-Reinforced Composites via Full Factorial Design. Composite Structure," *Compos. Struct.*, 2018.

[14] ASTM D3039/D3039M − 14 and Standard, "Standard Test Method for Tensile Properties of Polymer Matrix Composite Materials1," pp. 1–13, 2014.

[15] ASTM D790-15, "Standard Test Methods for Flexural Properties of Unreinforced and Reinforced Plastics and Electrical Insulating Materials. D790," pp. 1–12, 2015.

[16] ASTM International, "ASTM D7249/D 7249M - 12 Standard Test Method for Facing Properties of Sandwich Constructions by Long Beam Flexure," *Annu. B. ASTM Stand.*, vol. i, pp. 1–9, 2012.

[17] P. M. Materials, "Standard Test Method for Determining the Charpy Impact Resistance of Notched Specimens of Plastics 1," pp. 1–17, 2010.

[18] R. F. Gibson, "Principles of Composite Material Mechanics," *Isbn0070234515 9780070234512*, no. 205, p. xxvii, 579 p., 1994.

[19] G. B. Chai and P. Manikandan, "Low velocity impact response of fibre-metal laminates - A review," *Compos. Struct.*, vol. 107, pp. 363–381, 2014.

[20] J. C. Santos, R. L. Siqueira, L. M. G. Vieira, R. T. S. Freire, V. Mano, and T. H. Panzera, "Effects of sodium carbonate on the performance of epoxy and polyester coir-reinforced composites," *Polym. Test.*, vol. 67, no. January, pp. 533–544, 2018.

[21] J. Bieniaś, K. Majerski, B. Surowska, and P. Jakubczak, "THE MECHANICAL PROPERTIES AND FAILURE ANALYSIS," *Compos. Theory Pract.*, vol. 3, pp. 220–224, 2013.

[22] L. M. G. Vieira, J. Cesar, T. Hallak, J. Carlos, C. Rubio, and F. Scarpa, "Novel fibre metal laminate sandwich composite structure with sisal woven core," *Ind. Crop. Prod.*, vol. 99, pp. 189–195, 2017.

[23] F. D. Morinière, R. C. Alderliesten, and R. Benedictus, "Modelling of impact damage and dynamics in fibre-metal laminates - A review," *Int. J. Impact Eng.*, vol. 67, pp. 27–38, 2014.

[24] G. S. Dhaliwal and G. M. Newaz, "Experimental and numerical investigation of flexural behavior of carbon fiber reinforced aluminum laminates," *J. Reinf. Plast. Compos.*, vol. 35, no. 12, pp. 945–956, 2016.

[25] A. E. Hughes, J. M. C. Mol, and R. G. B. Editors, *Springer Series in Materials Science 233 Active Protective Coatings*. .